



Australian Journal of Earth Sciences

An International Geoscience Journal of the Geological Society of Australia

ISSN: (Print) (Online) Journal homepage: <https://www.tandfonline.com/loi/taje20>

The origin of mafic–ultramafic rocks and felsic plutons along the Clarke River suture zone: implications for porphyry exploration in the northern Tasmanides

A. Edgar, I. Sanislav & P. Dirks

To cite this article: A. Edgar, I. Sanislav & P. Dirks (2023): The origin of mafic–ultramafic rocks and felsic plutons along the Clarke River suture zone: implications for porphyry exploration in the northern Tasmanides, Australian Journal of Earth Sciences, DOI: [10.1080/08120099.2023.2234964](https://doi.org/10.1080/08120099.2023.2234964)

To link to this article: <https://doi.org/10.1080/08120099.2023.2234964>



© 2023 The Author(s). Published by Informa UK Limited, trading as Taylor & Francis Group.



Published online: 27 Jul 2023.



Submit your article to this journal [↗](#)






View related articles [↗](#)



View Crossmark data [↗](#)

The origin of mafic–ultramafic rocks and felsic plutons along the Clarke River suture zone: implications for porphyry exploration in the northern Tasmanides

A. Edgar , I. Sanislav  and P. Dirks 

College of Science and Engineering, Economic Geology Research Centre (EGRU), James Cook University, Townsville, Australia

ABSTRACT

The Clarke River Fault in northeast Queensland records an early Paleozoic history of subduction, accretion and continental suturing. Samples of mafic–ultramafic rocks collected proximal to the Clarke River Fault record oceanic geochemical affinities and comprise alteration assemblages consistent with an ophiolitic origin. The *ca* 456 Ma Falls Creek Tonalite records a continental-arc geochemical signature and was formed in response to long-lived subduction beneath the Thomson Orogen. Ordovician subduction beneath the Thomson Orogen is broadly coeval with arc magmatism documented in the Lachlan Orogen, which has been associated with the formation of several large porphyry ore deposits. The Falls Creek Tonalite yields adakite-like geochemical signatures that reflect a fertile melt source conducive to the formation of porphyry ore deposits. The outcropping plutons record ductile deformation consistent with mid-crustal depths, and they were emplaced during late syntectonic activity. This implies that the Falls Creek Tonalite was emplaced at too great a depth to have formed porphyry ore deposits. The northern Charters Towers Province shares many geological similarities to the Greenvale Province, where the erosional level may be shallower, and the potential for porphyry deposit formation and preservation may be greater.

KEY POINTS

1. Mafic–ultramafic rocks situated along the Clarke River Fault are of ophiolitic origin.
2. The Clarke River Fault is an early Paleozoic suture zone.
3. The northern Tasmanides contain adakitic plutons formed from hydrous, fertile melts, conducive to the formation of porphyry ore deposits.

ARTICLE HISTORY

Received 4 April 2023
Accepted 5 July 2023

KEYWORDS

magma fertility; ophiolites; porphyry deposits; suture zones; Tasmanides; tectonics

Introduction

Following the breakup of Rodinia and amalgamation of Gondwana, convergence along eastern Gondwana was accommodated by the widespread Terra Australis subduction system (Cawood, 2005). In Australia, the evolution of the Terra Australis Orogen has been recorded in the Tasmanides. Comparisons have been drawn between the Tasmanides and the Andean orogenic belt (Glen, 2013; Greenfield *et al.*, 2011), which hosts some of the world's largest porphyry Cu deposits (Mpodozis & Cornejo, 2012) such as the deposits in the Escondida district (>144 Mt of Cu; Hervé *et al.*, 2012) and the Rio Blanco deposit (1.257 Gt @ 0.57 wt% Cu; Chen *et al.*, 2022). Like in the Andes, the Tasmanides host a number of world-class porphyry Cu–Au deposits including the Cadia-Ridgeway orebodies (~50 Moz Au, ~9.5 Mt Cu; Harris *et al.*, 2020). These orebodies and other significant porphyry deposits are hosted within, or

occur proximal to, the Ordovician–Silurian Macquarie Arc of the Lachlan Orogen (Cooke *et al.*, 2007; Glen *et al.*, 2007). They are commonly gold-dominant and associated with shoshonitic volcanic centres and alkalic porphyry stocks. Similarities to the geology of the Macquarie Arc have been reported within the more northerly Thomson and Mossman orogens. These terranes all recorded evidence of broadly coeval, intra-oceanic-arc magmatism and collisional style tectonics (Edgar *et al.*, 2022a, 2022b; Henderson *et al.*, 2011). Despite the geological similarities between these terranes, comparable, large porphyry deposits have yet to be discovered in the northern Tasmanides.

Many of the most prolific Cu–Au producing porphyry belts contain ophiolite complexes (Glen *et al.*, 2012; Kuşçu *et al.*, 2019). Ophiolite complexes are variably sized, structurally interleaved lenses of mafic–ultramafic rocks with an oceanic affinity that have been tectonically emplaced onto continental crust during orogenesis (Dilek & Furnes, 2014). The

CONTACT A. Edgar  alexander.edgar@my.jcu.edu.au
Editorial handling: Chris Fergusson

© 2023 The Author(s). Published by Informa UK Limited, trading as Taylor & Francis Group.

This is an Open Access article distributed under the terms of the Creative Commons Attribution-NonCommercial-NoDerivatives License (<http://creativecommons.org/licenses/by-nc-nd/4.0/>), which permits non-commercial re-use, distribution, and reproduction in any medium, provided the original work is properly cited, and is not altered, transformed, or built upon in any way. The terms on which this article has been published allow the posting of the Accepted Manuscript in a repository by the author(s) or with their consent.

Cowley Ophiolite Complex (COC) in northeast Queensland is the first ophiolite sequence that has been described from the northern Tasmanides (Edgar *et al.*, 2022a). The COC was interpreted to have formed within a supra-subduction zone of an outboard, intra-oceanic-arc complex, which was later accreted to the continental margin. To date, the COC is the only confirmed ophiolite complex in the northern Tasmanides; however, other occurrences of mafic–ultramafic rocks with possible ophiolite affinities have been reported from several major structures in north Queensland (Arnold & Rubenach, 1976; Edgar *et al.*, 2022a).

The Clarke River Fault is a major structure that has been interpreted as a suture zone between the Thomson and Mossman orogens (Dirks *et al.*, 2021; Edgar *et al.*, 2022b). Along this fault zone, lenses of mafic–ultramafic rocks have been observed and occur in proximity to Ordovician oceanic amphibolite and metasediment (Dirks *et al.*, 2021). In this contribution, we investigate the petrogenesis of mafic–ultramafic rocks positioned along the Clarke River Fault to further constrain the tectonic setting of the northern Charters Towers Province. We then assess the magma fertility of the Falls Creek Tonalite and evaluate the potential for porphyry deposits within the region (Dirks *et al.*, 2021; Edgar *et al.*, 2022b).

Geological setting

The Paleozoic geological formations of eastern Australia have been subdivided into five distinct orogens, collectively known as the Tasmanides. Most geological scenarios for the development of the Tasmanides invoke long-lived, accretionary style tectonic models, in which continent growth has been attributed to a westward-dipping, and eastward migrating subduction complex, although some models have suggested periods of subduction polarity reversal (Aitchison & Buckman, 2012) and collisional style tectonics (Edgar *et al.*, 2022a). The Tasmanides in northeast Queensland comprise the Thomson and Mossman orogens (Figure 1a). Outcrops of the Thomson orogen are largely concealed by mid-Paleozoic to Cenozoic cover sequences; however, exposures of early Paleozoic rocks exist within the Greenvale and Charters Towers provinces. The rocks in these provinces have been interpreted as basin sequences that were deposited within a Paleozoic back-arc environment, and they unconformably overlie Neoproterozoic to Cambrian basement metasedimentary and meta-igneous rocks (Henderson *et al.*, 2020). The Charters Towers Province is bound to the north by the Clarke River Fault, and the Greenvale Province is bound to the north by the Lynd Mylonite Zone, an exposed portion of the North Australian Craton margin. To the south the Greenvale Province is truncated by the Burdekin River Fault (Fergusson *et al.*, 2007b; Withnall & Henderson, 2012).

The Mossman Orogen is a north–south-oriented, elongate belt of Ordovician–Devonian rocks situated northeast of the Thomson Orogen (Kumar *et al.*, 2022, 2023). The belt has

been subdivided into the Broken River Province to the south, and the Hodgkinson Province to the north (Figure 1). The Broken River Province consists of Ordovician–Devonian, active margin sequences, that contain volcano-sedimentary rocks, turbidite successions and tectonic melange (Henderson & Fergusson, 2019; Vos *et al.*, 2005). To the southeast, the Broken River Province is in tectonic contact with the Charters Towers Province along the Clarke River Fault. To the northeast, the Broken River Province bounds the Greenvale Province along the Burdekin River Fault.

The tectonic boundaries that delineate the Greenvale, Charters Towers and Broken River provinces coincide with the location of numerous ore deposits and mineral prospects. However, the nature of these boundaries, and their relationships to tectonic processes, are not well understood. The Burdekin River Fault Zone, and the associated Nickel Mine Fault, Halls Reward Fault and Gray Creek Fault are thought to control the distribution of mafic–ultramafic complexes, which underly the lateritic Ni–Co–Sc deposits in the Greenvale region (Arnold & Rubenach, 1976). These ultramafic complexes, which include the Sandalwood, Boiler Gully and Gray Creek complexes, are situated proximal to the Burdekin River Fault Zone, and are probably of ophiolitic origin. They mostly consist of amphibolite, and serpentinised peridotite of dunitic to pyroxenitic composition (Arnold & Rubenach, 1976; Withnall *et al.*, 1988). The Balcooma Metamorphics, situated within the Greenvale Province, are bounded to the north by the Lynd Mylonite Zone. Numerous VMS style Pb–Zn deposits occur within the Balcooma Metamorphics and within proximity of the Lynd Mylonite Zone (Huston *et al.*, 1992).

Positioned along the Clarke River Fault, the Ordovician, Running River Metamorphics comprise strongly deformed, amphibolite facies rocks, which are mostly composed of amphibolite, felsic gneiss and quartzite (Figure 1b). The sequence was intruded by the Falls Creek Tonalite at 456 Ma (Dirks *et al.*, 2021). Dirks *et al.* (2021) have interpreted the Running River Metamorphics as obducted oceanic crust, which was structurally juxtaposed against basement consisting of S-type granitic gneiss. Metamorphic diamonds have been found within almandine–spessartine garnet-bearing quartzite from the Running River Metamorphics (Edgar *et al.*, 2022b), which indicates that the Running River Metamorphics experienced ultra-high-pressure metamorphism at pressures >3.5 GPa and temperatures >850 °C (Edgar *et al.*, 2022b). The presence of UHP rocks, coupled with the tectonic position of the Running River Metamorphics along a major regional structure, indicates that the Clarke River Fault represents a suture zone between the Charters Towers and Broken River provinces (Edgar *et al.*, 2022b).

Sample descriptions

The Running River Metamorphics contain felsic to ultramafic, meta-igneous lithologies that include tonalite,

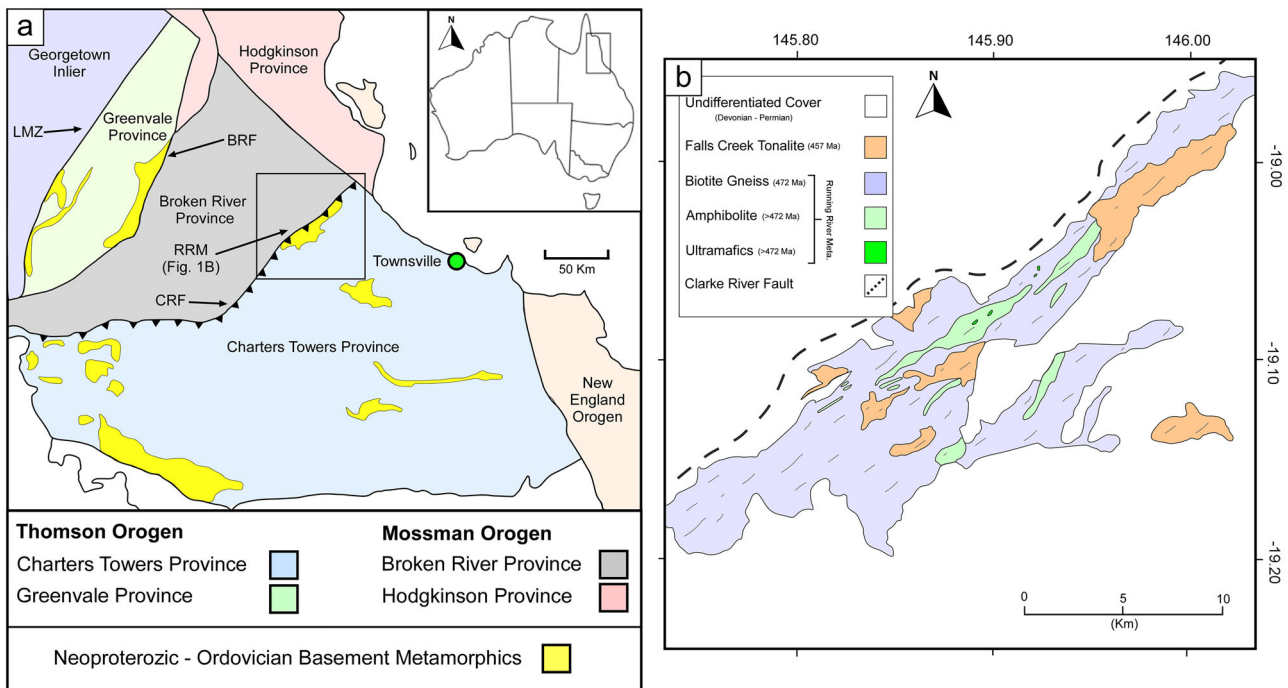


Figure 1. (a) Tectonic framework of the northeastern Tasmanides after Edgar *et al.* (2022b). The black box highlights the location of the Running River Metamorphics; one of many early Paleozoic, basement terranes in north Queensland. CRF, Clarke River Fault; LMZ, Lynd Mylonite Zone; BRF, Burdekin River Fault; RRM, Running River Metamorphics. (b) Geological map of the Running River Metamorphics after Dirks *et al.* (2021).

hornblende, amphibolite, anthophyllite schist, amphibole pegmatite and chlorite schist.

Hornblende

Coarse-grained hornblende occurs over tens of metres in outcrops and subcrops, with poorly exposed contact zones. The hornblende is typically fresh and contains >90 vol% coarse-grained hornblende, with minor chlorite veinlets and ilmenite (Figure 2g). It can be distinguished from the more common and regionally distributed amphibolite unit described by Dirks *et al.* (2021), by the absence of plagioclase and a coarse, equigranular texture. Ilmenite commonly occurs within chlorite veinlets, or as exsolution needles within hornblende (Figure 2h).

Anthophyllite schist

Anthophyllite schist has been sampled from two localities within the Running River Metamorphics where it occurs as tens of metre-scale lenses within larger blocks of amphibolite. Samples were collected from outcrop and subcrop; however, field relationships with the surrounding rock units are not clear owing to poor exposure. Anthophyllite schist contains >90 vol% fine- to medium-grained, fibrous to prismatic anthophyllite (Figure 2a, e, f), with minor coarse-grained hornblende and variable proportions of disseminated chromite, which can reach up to 10 vol% in hand samples. Fresh anthophyllite schist is pale green in colour, whereas weathered varieties are reddish brown.

Chlorite schist

A single sample of chlorite schist was collected from within a larger lens of amphibolite, and it occurs as a well-exposed, metre-wide outcrop. Chlorite schist contains large grains of magnesio-hornblende embedded within a fine-grained chlorite–chromite matrix. Chromite commonly occurs as fine, disseminated granules within the relict cores of large, prismatic, ferro-magnesian-silicate grains, that have altered to chlorite. The relict ferro-magnesian-silicate grains commonly contain >20 vol% chromite, which may indicate extremely Cr-rich compositions prior to alteration.

Amphibolite

Samples of amphibolite were collected from outcrops and subcrops proximal to the ultramafic lithologies. The amphibolite is dark green to black in colour, strongly linedated, medium to coarse-grained, and it contains 60–90 vol% amphibole, 10–30 vol% plagioclase and accessory opaque phases. The amphibole species consists predominantly of magnesian hornblende to ferromagnesian hornblende (online data).

Amphibole pegmatite

An outcrop of pegmatite-like amphibolite was sampled from the southwestern extent of the Running River Metamorphics. The outcrop comprises mafic–intermediate rocks that contain highly variable proportions of feldspar (0–60 vol%) and amphibole (40–100 vol%). The outcrop is

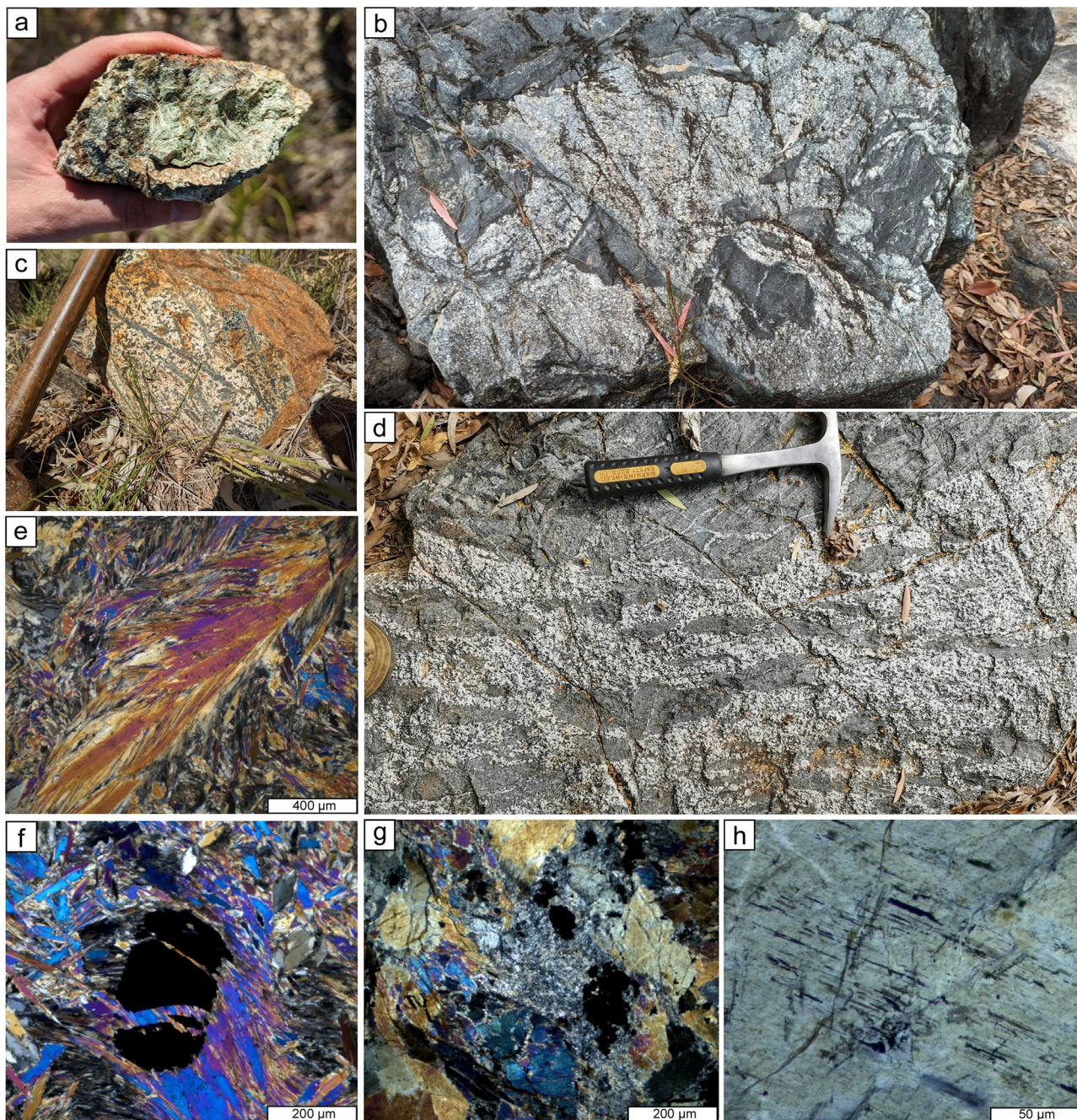


Figure 2. Compilation of field photographs and photomicrographs. (a) Hand sample of fibrous, green, anthophyllite schist displaying a radial crystal habit, characteristic of anthophyllite schist from the Running River Metamorphics. (b) Outcrop photo depicting the intrusive relationships between the Falls Creek Tonalite and polydeformed amphibolite rafts. (c) Outcrop photo of a feldspar-dominant pegmatite with large, hornblende megacrysts. (d) Outcrop photo depicting the relationships between a channel of partial melt material (leucosome) in which are raft blocks of the parent amphibolite and crosscuts deformation fabrics. (e) Photomicrograph of coarse-grained, fibrous, anthophyllite schist. (f) Photomicrograph of anthophyllite schist with a large, deformed, chromite grain. (g) Photomicrograph of coarse-grained hornblende with zones of chlorite veining and interstitial ilmenite (opaque). (h) Photomicrograph of hornblende focussing on the core of a hornblende crystal. The core contains oriented exsolution of Ti-oxides.

texturally heterogenous, with zones of massive, coarse-grained amphibole, as well as feldspar-dominant zones with needle like amphibole phenocrysts that are >15 cm in length (Figure 3c). The most amphibole-rich (>90 vol% hornblende) portions of the pegmatite body were sampled for geochemistry to compare with the hornblende samples. Field relationships of this unit with the

surrounding Running River Metamorphics are obscured by a shallow cover.

Falls Creek Tonalite

The Falls Creek Tonalite occurs as a series of northeast-trending, kilometre-scale, intrusive bodies, which are best

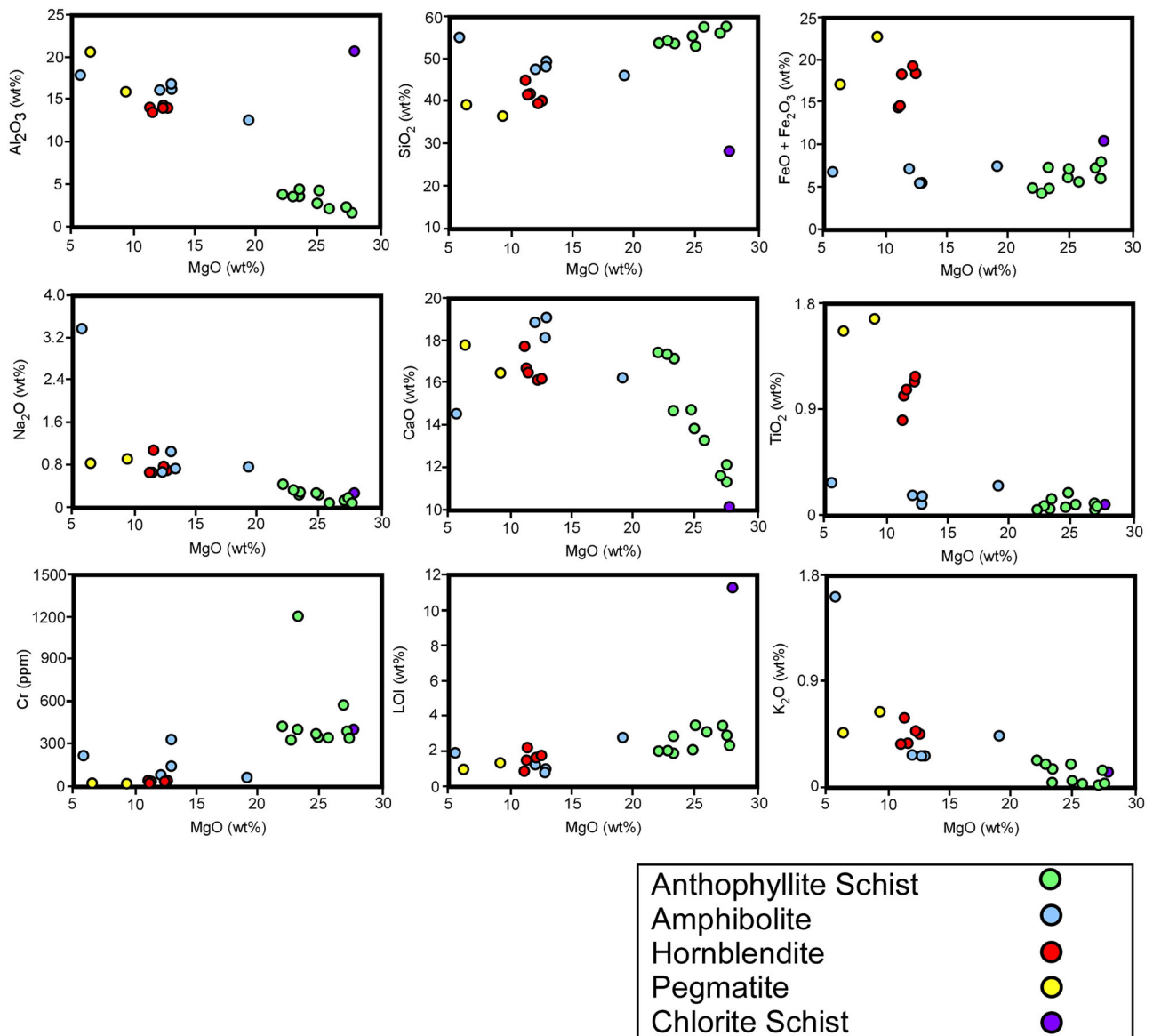


Figure 3. Major elements vs MgO (wt%) for the mafic–ultramafic lithologies collected from Running River.

exposed in the southwestern Running River Metamorphics and within the Running River riverbed (Dirks *et al.*, 2021). The Falls Creek Tonalite consists of coarse-grained, equigranular, quartz and plagioclase, with minor biotite, orthoclase and hornblende, and it ranges in compositions from tonalite to granodiorite. On the basis of geochemistry, Dirks *et al.* (2021) suggested that the Falls Creek Tonalite had formed within a continental-arc setting. The Falls Creek Tonalite intruded the Running River Metamorphics (Figure 2b) but is crosscut by later, *in situ* partial melt (leucosome) segregated from the amphibolite (Figure 2b, d).

Methods

Twenty-three samples of mafic–ultramafic rocks and eight samples of the Falls Creek Tonalite were collected from the Running River Metamorphics to conduct whole-rock major

and trace-element geochemistry, mineral geochemistry and petrographic analyses. Petrographic thin-sections were prepared at Ingham Petrographics and analysed at James Cook University. Major-element geochemistry was carried out using an XRF housed in the Advanced Analytical Centre at James Cook University, Townsville. Trace-element geochemistry was analysed using an LA-ICP-MS housed within the same facility. Two separate laser ablation experiments were conducted; the first to analyse the ultramafic rocks and the second to analyse the Falls Creek Tonalite. Laser conditions were set at 3 J/cm² with a spot size of 110 μm. Standards used in the analysis of ultramafic rocks and tonalite included GSE_1G, BCR2G, BHVO2G, GSD1G, NIST610 and NIST612. The raw data were processed with lolite 4 software.

Twenty major-element analyses of chromite were collected on the JEOL JXA 8200 electron probe micro-analyser

(EPMA), hosted within the same facility, using an acceleration voltage of 15 kV, a 2 nA probe current and a probe diameter of 5 μm .

Results

Whole-rock major-element geochemistry

The hornblendite samples are chemically homogeneous. They contain 11–13 wt% MgO, 39–45 wt% SiO₂, 13–15 wt% Al₂O₃, 17–20 wt% total FeO, 9–13 wt% CaO, 0.8–1.2 wt% TiO₂, 0.6–1.1 wt% Na₂O, 0.3–0.6 wt% K₂O and 0.01–0.04 wt% Cr₂O₃ (Figure 3; online data). The hornblendite samples plot as subalkaline basalts (Figure 4a). They fall along the tholeiitic trend on the AFM diagram (Figure 4b; Irvine & Baragar, 1971; Kuno, 1968), across the continental-arc basalt (CAB) and island-arc tholeiite (IAT) fields of the oceanic basalt ternary discrimination plot (Figure 4c; Mullen, 1983) and within the low-Ti island-arc basalt (IAB) of the Ti vs V discrimination plot (Figure 4d; Shervais, 1982). The hornblendite samples plot outside the discriminatory fields for the Ti vs Zr (Pearce & Cann, 1973) and Th/Yb vs Nb/La discrimination plots (Figure 4e, f; Pearce, 2008). The hornblendite samples display flat chondrite-normalised rare earth element (REE) patterns, with flat to weakly negative Eu anomalies (Figure 5).

The anthophyllite schist samples show linear variation in major-element composition. They contain 22–28 wt% MgO, 52–58 wt% SiO₂, 1–5 wt% Al₂O₃, 4–8 wt% total FeO, 2–12 wt% CaO, 0–0.2 wt% TiO₂, 0–0.5 wt% Na₂O, 0–0.3 wt% K₂O and 0.2–1 wt% Cr₂O₃ (Figure 3; online data). The anthophyllite schist samples plot as subalkaline basalt to basaltic-andesite (Figure 4a). The samples plot along the tholeiitic to calc-alkaline transition (Figure 4b) and within the continental-arc (Figure 4c, d), oceanic-arc (Figure 4d) and low-Ti IAB discriminatory fields (Figure 4f). The anthophyllite schist samples display variable chondrite-normalised REE patterns, with variable, positive and negative, Ce and Eu anomalies (Figure 5).

The chlorite schist sample contains 28 wt% MgO, 28 wt% SiO₂, 21 wt% Al₂O₃, 10 wt% total FeO, 0.2 wt% CaO, 0.1 wt% TiO₂, 0.3 wt% Na₂O, 0.1 wt% K₂O and 0.3 wt% Cr₂O₃ (Figure 3), and it plots within the subalkaline, basalt field (Figure 4a). The sample falls along the tholeiitic to calc-alkaline transition (Figure 4b) and plots within the CAB (Figure 4c), overlapping continental-arc and oceanic-arc and low-Ti IAB discriminatory fields (Figure 4). The chlorite schist sample displays a relatively flat chondrite-normalised REE pattern, with a strong, negative Eu anomaly and a depletion in Yb and Lu (Figure 5).

The major-element chemistry of the Running River Metamorphics amphibolite is heterogeneous. The samples collected in this study contain 5–20 wt% MgO, 45–55 wt% SiO₂, 12–18 wt% Al₂O₃, 5–8 wt% total FeO, 7–15 wt% CaO, 0.1–0.3 wt% TiO₂, 0.6–3.4 wt% Na₂O, 0.2–1.7 wt% K₂O and 0–0.3 wt% Cr₂O₃ (Figure 3; online data). The amphibolite samples from this study plot within the subalkaline, basalt

to basaltic-andesite field. They fall within the calc-alkaline, and tholeiitic trends, and plot within the CAB, island-arc and low-Ti IAB discriminatory fields (Figure 4). The amphibolite samples collected in this study mostly display LREE depleted chondrite-normalised signatures without an Eu anomaly (Figure 5).

The pegmatite samples contain 6–10 wt% MgO, 36–40 wt% SiO₂, 16–21 wt% Al₂O₃, 17–23 wt% total FeO, 10–13 wt% CaO, 1.5–1.7 wt% TiO₂, 0.8–1 wt% Na₂O and 0.4–0.7 wt% K₂O (Figure 3; online data). Pegmatite samples plot within the subalkaline, basalt field. They fall within the tholeiitic trend and plot within the IAT, NMORB and IAT/MORB discriminatory fields (Figure 4). The pegmatite samples display flat chondrite-normalised REE patterns with weakly negative Eu anomalies (Figure 5).

Samples of the Falls Creek Tonalite contain 0–3 wt% MgO, 64–73 wt% SiO₂, 16–19 wt% Al₂O₃, 0–5 wt% total FeO, 1–4 wt% CaO, 0–0.5 wt% TiO₂, 3–5 wt% Na₂O and 0.8–3 wt% K₂O (Figure 3; online data). The tonalite samples plot within the subalkaline–alkaline, intermediate-evolved, rhyodacite–trachy-andesite fields (Figure 4). The Falls Creek Tonalite display HREE-depleted chondrite-normalised REE patterns and record both positive and negative Eu anomalies (Figure 5).

Chromite chemistry

The chemistry of chromite grains from anthophyllite schist samples was measured to fingerprint the petrogenesis and tectonic setting of the mafic–ultramafic rocks within the Running River Metamorphics. Twenty analyses of chromite grains were collected from a single anthophyllite schist sample (online data). Chromite analyses were taken from grain cores and grain rims following major-element mapping (online data). Chromite grains from the anthophyllite schist are chemically homogeneous from core to rim. They contain 40–49 wt% Cr₂O₃, 16–24 wt% Al₂O₃ (an outlier at 13.7 wt% Al₂O₃), 28–30 wt% FeO, 5–9 wt% MgO, 0–2 wt% ZnO, >0.3 wt% TiO₂, Cr# 53–71 and Mg# 26–40.

The ratio of 3⁺ cations has been used to classify spinel minerals, fingerprint metamorphic modification and differentiate the petrogenetic setting of the host lithologies (Barnes & Roeder, 2001; Proenza *et al.*, 2008). Chromite grains from anthophyllite schist plot within the overlapping ophiolite complexes and stratiform-style complexes petrogenetic fields (Figure 6a). The chromite grains fall within the Al-chromite classification field and mostly within the lower-amphibolite-facies metamorphism field (Figure 6b).

The Cr# vs Mg# petrogenetic discrimination plots (Dick & Bullen, 1984) have been used to differentiate among chromite formed within abyssal peridotite, alpine peridotite, stratiform-type complexes and Alaskan-type complexes. Half of the chromite analyses from the anthophyllite schist plot within the overlapping Alaskan-type and stratiform-type fields, while the other half plot

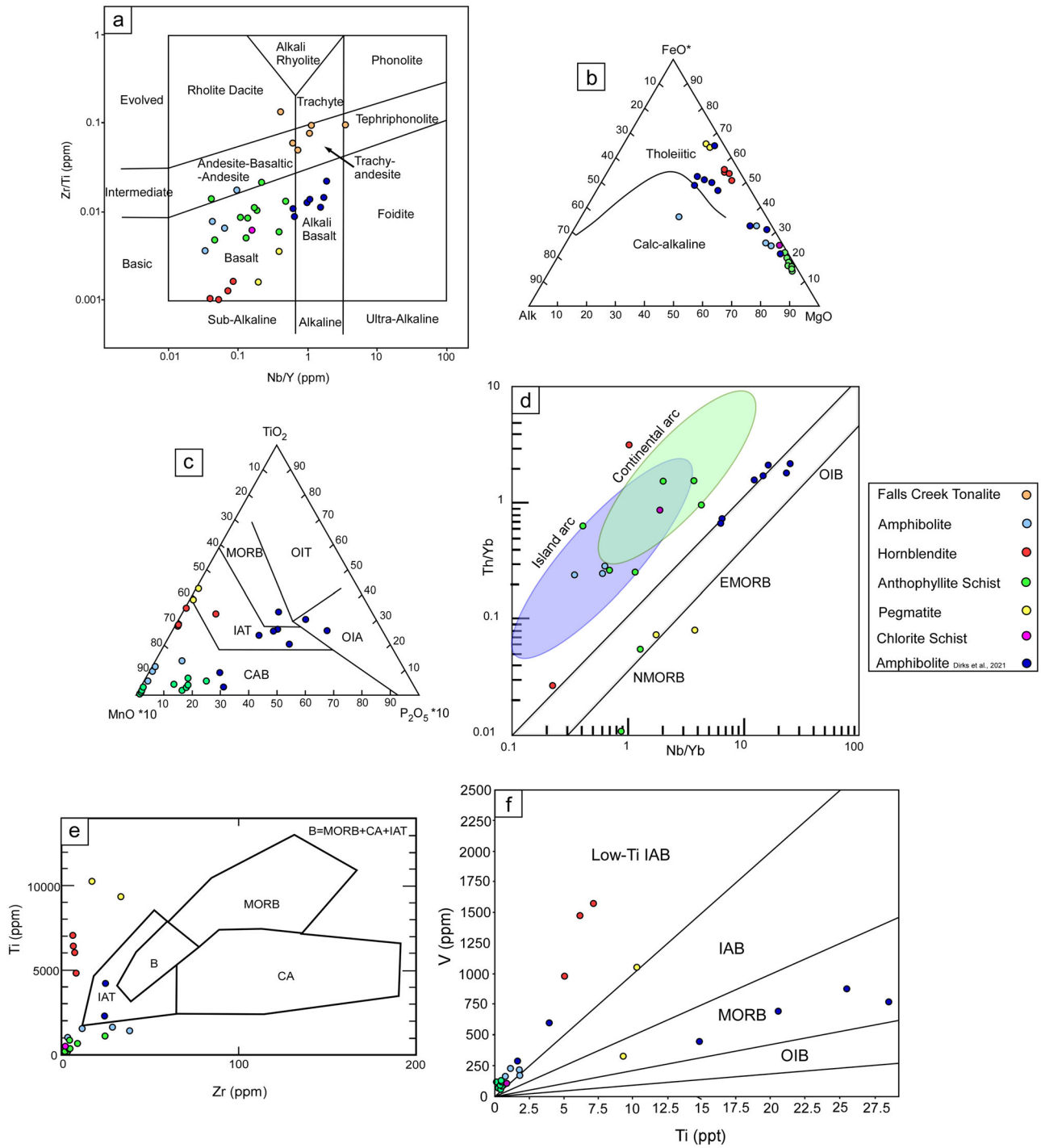


Figure 4. Geochemical, tectonic discrimination and classification plots for the rocks collected in this study with additional amphibolite samples collected by Dirks *et al.* (2021). (a) Immobile element rock classification after Winchester and Floyd (1977). (b) AFM ternary diagram after Irvine and Baragar (1971) and Kuno (1968). (c) Oceanic basalt ternary plot after Mullen (1983). (d) Th/Yb vs Nb/Yb MORB array plot after Pearce (2008) and Buckman *et al.* (2018). (e) Ti vs Zr plot after Pearce and Cann (1973). (f) V vs Ti plot after Shervais (1982).

outside the discriminatory fields (Figure 6c). The data points display a strong, positive, linear correlation between increasing Cr# and decreasing Mg#.

The TiO₂ vs Al₂O₃ geochemical discrimination plot of Kamenetsky *et al.* (2001) can be used to characterise spinels formed within various tectonic settings including

arcs, supra-subduction zones, back-arc basins, LIP's, spreading centres (MORB) and intraplate (OIB) locations. The chromite analyses from the anthophyllite schist plot as a weakly clustered group across the MORB, back-arc basin and supra-subduction zone tectonic discrimination fields (Figure 6d).

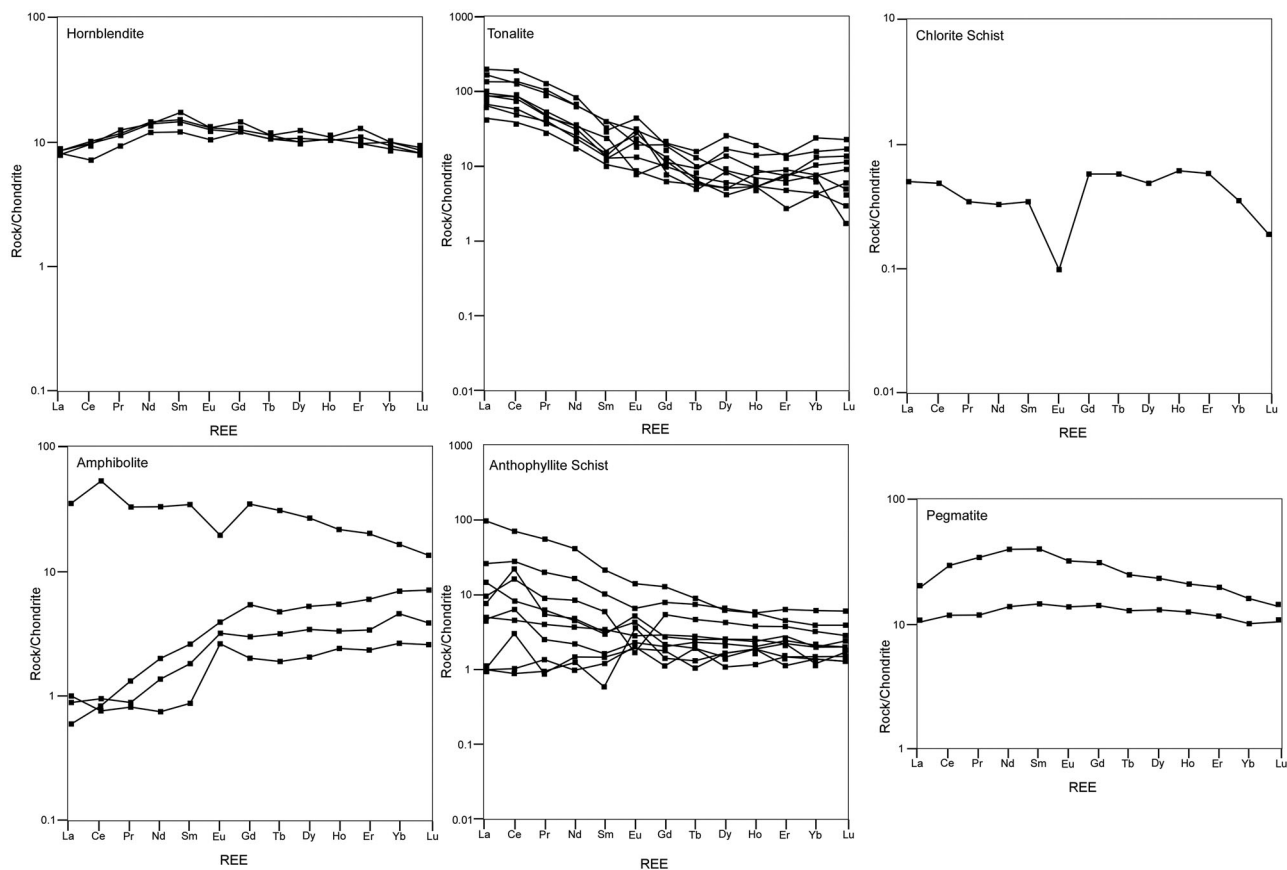


Figure 5. Chondrite-normalised (McDonough & Sun, 1995) REE plots for mafic-ultramafic samples, and tonalite samples collected in this study. Raw data recorded in the online data.

Discussion

Tectonic setting of the Running River mafic-ultramafic rocks

The dominant alteration styles observed within mafic-ultramafic rocks at Running River include ‘blackwall’ chlorite alteration and anthophyllite alteration. Blackwall chlorite alteration is the complete replacement of ferromagnesian silicate minerals by chlorite. It is an alteration style that typically occurs within subduction zone environments (Edgar *et al.*, 2022a; King *et al.*, 2003; Spandler *et al.*, 2008) whereby hydrothermal or metasomatic fluids, liberated from hydrous silicate minerals during prograde metamorphism, interact with magnesium-rich, ultramafic protoliths in the overriding mantle wedge (Zheng *et al.*, 2016). A similar model has been proposed to describe anthophyllite alteration, in which ferromagnesian pyroxene is completely replaced by anthophyllite, commonly under amphibolite facies conditions (Abdel-Karim *et al.*, 2016; Edgar *et al.*, 2022a; Yu *et al.*, 2019). Similar styles of alteration have been described by Edgar *et al.* (2022a) within the COC, which was interpreted as an ophiolite complex formed within an intra-oceanic supra-subduction zone setting, which was later accreted to the Australian continent along the Russell-Mulgrave Fault. The anthophyllite schist samples from Running River and the COC record mainly positive Eu

anomalies (Figure 5), which may reflect suppressed plagioclase fractionation resulting from the circulation of hydrous, subduction-related fluids (Müntener *et al.*, 2001). The similarities in alteration styles recorded by the COC and Running River ultramafic rocks may indicate a genetic link.

The amphibolite and hornblendite samples contain the lowest LOI contents and represent the least altered mafic-ultramafic rocks in the study area (Figure 3, LOI). These rocks record tholeiitic to calc-alkaline signatures and preserve predominantly MORB, IAT and oceanic-arc geochemical affinities (Figure 4). Mafic rocks recording tholeiitic to calc-alkaline compositions have been described in evolving intra-oceanic-arc settings (Belyaev *et al.*, 2021; George *et al.*, 2004; Klausen *et al.*, 2017). Along subduction margins, series of mafic-ultramafic rocks with calc-alkaline, IAT chemistry have been interpreted as supra-subduction zone ophiolite complexes (Buckman *et al.*, 2018; Yellappa *et al.*, 2010). On the other hand, the chondrite-normalised REE patterns for the amphibolite samples collected in this study are similar to N-MORB, which is characterised by a depletion in LREE and relative enrichment in HREE (Miao *et al.*, 2008; Sun *et al.*, 1979; Viereck *et al.*, 1989). We suggest that the combination of MORB, IAT and OIB (Dirks *et al.*, 2021) geochemical signatures recorded in the Running River amphibolites reflect an oceanic signature. Coexisting assemblages of MORB and subduction-related

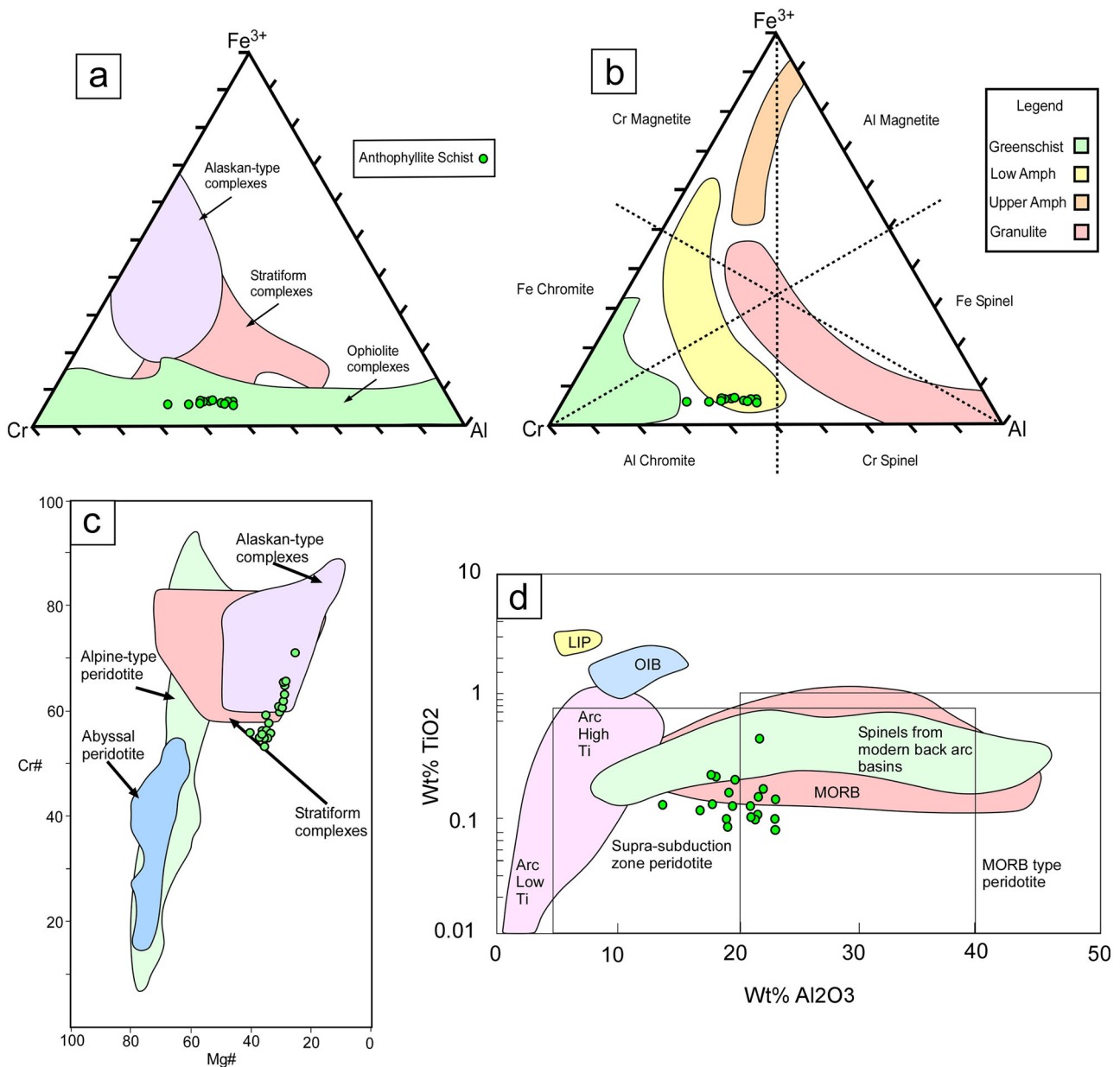


Figure 6. Compilation of geochemical, tectonic discrimination and classification plots for chromite hosted within anthophyllite schist from Running River. (a) Petrogenetic discrimination ternary diagram after Barnes and Roeder (2001) and Yu *et al.* (2019). (b) Metamorphic facies discrimination and chromite classification plot after Proenza *et al.* (2008). (c) Cr# vs Mg# after Dick and Bullen (1984). (d) TiO₂ vs Al₂O₃ after Kamenetsky *et al.* (2001).

mafic–ultramafic complexes are commonly recorded within collisional terranes and along suture zones (Buckman *et al.*, 2018; Liu *et al.*, 2018; Yao *et al.*, 2014).

Chromite chemistry

The chemistry of chromite grains from the anthophyllite schist is consistent with an ophiolitic, subduction-related source (Figure 6; Yu *et al.*, 2019). This is also consistent with the alteration and whole-rock geochemistry of mafic–ultramafic rocks in this study. However, while the chemistry of the chromite suggests significant metasomatic or metamorphic modification, such as low Mg:Fe ratios and Zn enrichment (online data; Barnes, 2000), the textures suggest

a lack of alteration. Chemical zonation of major elements is common in primary chromite modified by later hydrothermal or metasomatic fluids (Barnes, 2000; Colás *et al.*, 2014; Gamal El Dien *et al.*, 2019). Chromite grains from the anthophyllite schist lack significant, major-element zonation from core to rim (online data). However, they contain significantly lower Mg/Fe ratios than typical ophiolitic chromite (Dick & Bullen, 1984). Chromite grains with similar textural and chemical characteristics have been reported for the Oman ophiolite (Arai & Akizawa, 2014), and these were interpreted as crystallising directly from hydrothermal or metasomatic fluids. The protolith to the anthophyllite schist was most likely a pyroxenite (Abdel-Karim *et al.*, 2016), containing chromium-bearing pyroxene (Shiraki, 1997). We suggest,

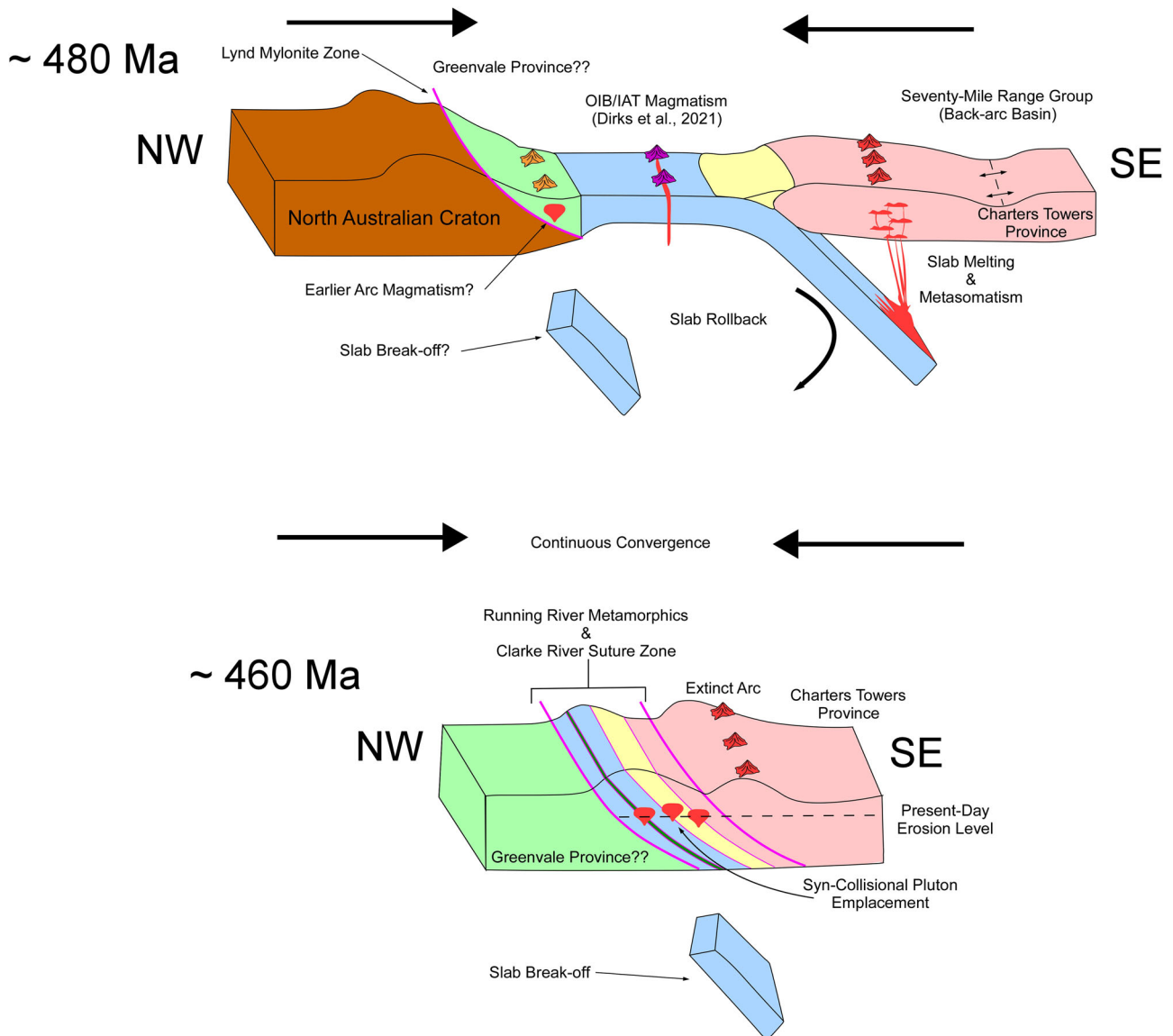


Figure 7. Proposed model depicting the early Paleozoic tectonic evolution of the northern Thomson Orogen. At *ca* 480 Ma, southeastward-dipping subduction of oceanic crust below the continental Charters Towers Province evokes arc magmatism and back-arc basin extension. Convergence, slab roll-back and westwards slab retreat gradually close an ocean basin separating the Charters Towers Province from the North Australian Craton. As a result of continuous convergence along the eastern Gondwana margin, by *ca* 460 Ma, the Charters Towers Province collides with the Greenvale Province (or North Australian Craton), resulting in ophiolite emplacement and continent suturing along the Clarke River Suture Zone. The Falls Creek Tonalite intrudes the Running River Metamorphics during late syndeformation, inheriting arc-like geochemical signatures from prior slab melting and mantle wedge metasomatism.

that during metasomatic alteration of the pyroxenite protolith, chromium was liberated from pyroxene during recrystallisation to anthophyllite, and it was later incorporated within Mg-depleted, metasomatic chromite.

Tectonic setting and magma fertility of the Falls Creek Tonalite

The *ca* 456 Ma, I-type, Falls Creek Tonalite is a silica-rich, calc-alkaline, syntectonic pluton suite of continental-arc affinity (Dirks *et al.*, 2021). This magmatic belt is situated southeast of, and parallel to, the Clarke River Fault (suture), and it probably formed in response to southeastwards facing subduction below the Charters Towers Province

(Thomson Orogen; Figure 7; Edgar *et al.*, 2022a, 2022b). Evidence for early Paleozoic, Thomson Orogen-facing subduction has been recorded by the Cambro-Ordovician Seventy Mile Range Group, which was interpreted as an east–west-trending, back-arc basin assemblage, deposited atop of continental crust (Henderson, 1986). Our interpretation of an approximately northeast–southwest-trending subduction complex, and associated magmatism, provides an alternative explanation for the east–west trend of the Seventy Mile Range Group back-arc basin and its distal position to the northern margin of the Charters Towers Province (Figure 7).

Ordovician, subduction-related magmatism in the northern Charters Towers Province was broadly coeval with

intra-oceanic-arc magmatism in the Lachlan Orogen, which was associated with the formation of the Macquarie Arc (Aitchison & Buckman, 2012; Crawford *et al.*, 2007) and associated giant porphyry deposits. Most tectonic models detailing the tectonic setting of the Macquarie Arc depict a westward-dipping (continent-facing) subduction complex and a magmatic arc that developed atop of an extended oceanic margin (Glen *et al.*, 2016; Murphy *et al.*, 2011). Alternative models invoke an eastward-dipping (ocean-facing) intra-oceanic subduction system, which, during westward slab retreat, transported an exotic island-arc complex that collided with the eastern Gondwana margin (Aitchison & Buckman, 2012; Zhang *et al.*, 2019).

Prolonged, eastward-dipping subduction of oceanic crust and terrane collision, as described by Aitchison and Buckman (2012) in the Lachlan Orogen, is similar to the tectonic setting suggested by Edgar *et al.* (2022b) for the northern Thomson Orogen. Despite the subduction-related magmatic arcs of the Lachlan Orogen being host to numerous large deposits, the synchronous, along-strike, magmatic arcs of the northern Thomson Orogen have received relatively little attention. Magmatic arcs of the northern Thomson Orogen may be a favourable environment for the formation of porphyry ore deposits.

Several geochemical fertility tools have been proposed to assist in fingerprinting favourable conditions conducive to the formation of porphyry deposits. Sr/Y ratios in felsic-intermediate magmatic rocks have been interpreted to constrain the magmatic water content (Chiaradia *et al.*, 2012; Richards, 2011). During melt fractionation, a high magmatic water content promotes amphibole fractionation while suppressing plagioclase fractionation, thereby enriching the melt in Al and Sr, while depleting it in Y until eventual plagioclase saturation (Loucks, 2014). However, fertility analysis of Sr/Y ratios requires relatively unaltered samples, owing to Sr mobility during alteration (Wells *et al.*, 2021). Zr is an immobile element that saturates at lower temperatures within hydrous melts compared with dry melts. Zr has been used as an alternative to Sr in altered magmatic rocks (Wells *et al.*, 2021). Porphyry-style mineralisation is commonly associated with adakitic magmatism (Richards & Kerrich, 2007; Sun *et al.*, 2011). Adakite is a variety of subduction-related melt characterised by >56 wt% SiO₂, >15 wt% Al₂O₃, <18 ppm Y, <1.9 ppm Yb and >400 ppm Sr (Defant & Drummond, 1990). Adakitic magmas typically display high Sr/Y and high LREE/HREE ratios controlled by amphibole and garnet fractionation, respectively.

Geochemical analysis (Figure 8) of the Falls Creek Tonalite indicates that it was derived from an evolved magma with a high magmatic water content, which underwent prolonged amphibole fractionation. In addition to the high Sr/Y and low Zr concentrations, most samples of the Falls Creek Tonalite record a positive Eu anomaly, indicative of plagioclase suppression under hydrous conditions (Richards *et al.*, 2012). The Falls Creek Tonalite records adakite-like signatures with high SiO₂, high Al₂O₃, low MgO,

high Sr/Y and, in some samples, high La/Yb ratios. Adakite-like signatures have been interpreted to record a range of processes including subduction-related deep melting of eclogite (Moyen, 2009), collision-related partial melting of the lower crust (Chung *et al.*, 2003), partial melting of underplated mafic crust (Petford & Atherton, 1996) and fractionation of normal, calc-alkaline series, arc magmas (Richards & Kerrich, 2007; Sun *et al.*, 2013). Subduction-related melting of a residual garnet source would likely produce a melt more strongly depleted in HREE relative to LREE than what is recorded in the Falls Creek Tonalite (Rapp *et al.*, 1991; Xiong *et al.*, 2006). Alternatively, syn or post-collisional melts, which were preceded by extended periods of oceanic subduction, may record subduction-related signatures (Sajona *et al.*, 2000). Dirks *et al.* (2021) described steep, isoclinal, reclined folds within the Falls Creek Tonalite that they correlated to the D₄ deformation event, which affected the Running River Metamorphics suggesting a syntectonic emplacement (Figure 7).

Evidence for a post-tectonic extensional event following terrain suturing along the Clarke River Fault has been suggested based on *in situ*, decompression partial melting of amphibolite (Dirks *et al.*, 2021). The partial melt, which was dated at ca 436 Ma, is undeformed and crosscuts all of the earlier compressional fabrics in the Running River Metamorphics and Falls Creek Tonalite. Based on the age of the partial melt, this extensional event occurred after ca 450 Ma and may represent a period of post-collisional, orogenic collapse (Dewey, 1988; Song *et al.*, 2014), following continental suturing along the Clarke River Fault.

Porphyry deposit preservation in the northern Tasmanides

Porphyry deposits are emplaced within the upper crust, commonly between 2 and 5 km (Sillitoe, 2010). The Running River Metamorphics, which host the Falls Creek Tonalite intrusions, record widespread amphibolite facies metamorphism, associated with mid-crustal depths assuming a normal geotherm (Zheng & Chen, 2017). The Falls Creek Tonalite intruded the Running River Metamorphics at ca 456 Ma and experienced at least two ductile deformation events suggesting that emplacement occurred at mid-crustal depths (Figure 7; Dirks *et al.*, 2021). Although the Falls Creek Tonalite exhibits many geochemical characteristics of a magma derived from an evolved, fertile source, the mapped bodies have been emplaced too deeply to have formed porphyry-style mineralisation. Potential for mineralisation exists further to the southeast, where the Running River Metamorphics, and presumably the Falls Creek Tonalite, were intruded, and overlain by, Carboniferous–Permian magmatic rocks of the Kennedy Igneous Association. Deposition of this volcanic cover sequence atop of early Paleozoic crust (Running River Metamorphics) could have occurred prior to deep erosion,

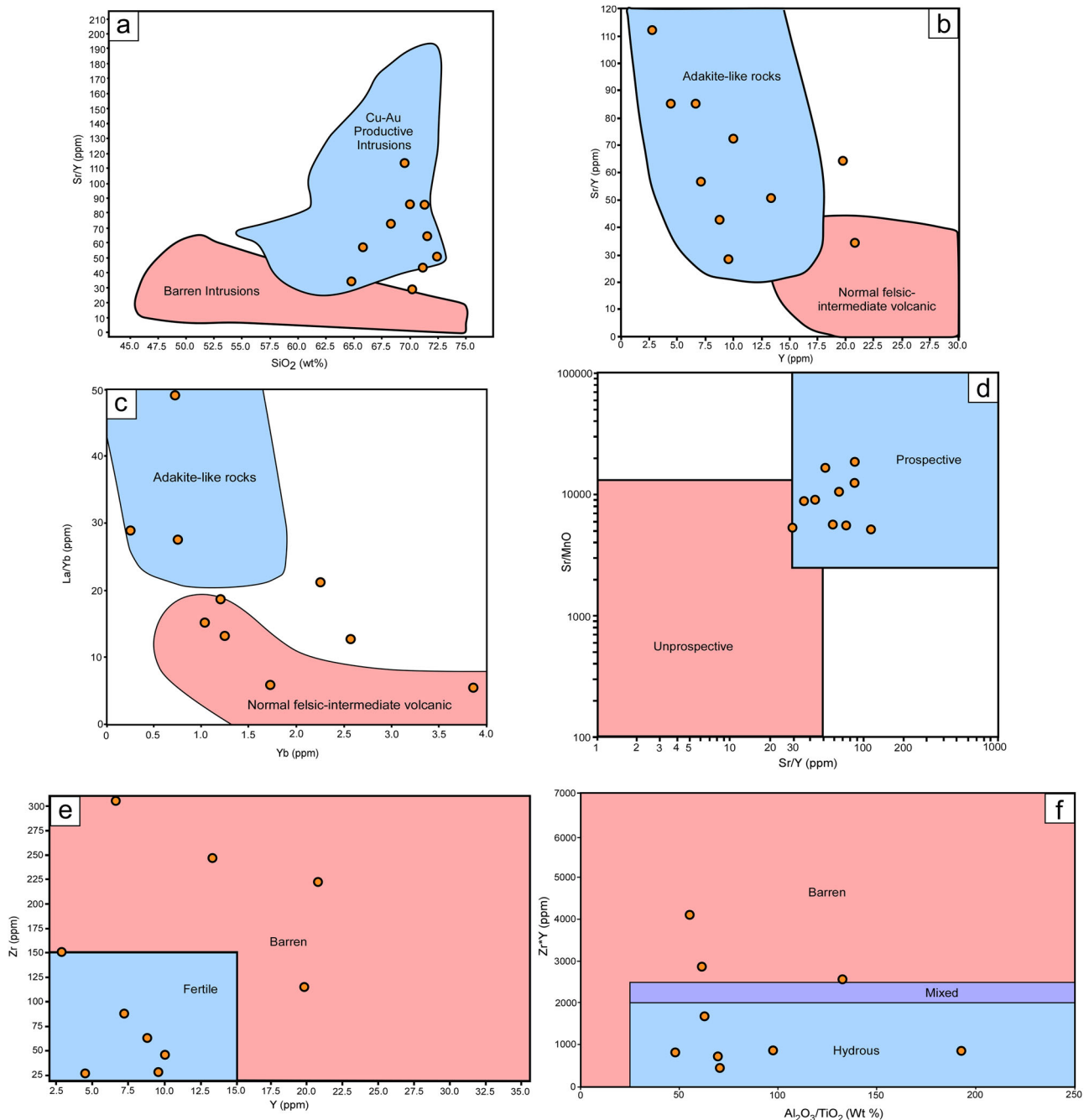


Figure 8. Falls Creek Tonalite whole-rock geochemistry plotted across a compilation of magma fertility discrimination diagrams. (a) Sr/Y vs SiO₂ after Loucks (2014). (b) Sr/Y vs Y after Defant and Drummond (1993). (c) La/Yb vs Yb after Castillo *et al.* (1999). (d) Sr/MnO vs Sr/Y after Wells *et al.* (2021). (e) Zr vs Y after Wells *et al.* (2021). (f) Zr*Y vs Al₂O₃/TiO₂ after Wells *et al.* (2021). Samples collected in this study and from Dirks *et al.* (2021).

and thus shallower level intrusions of similar age to the Falls Creek Tonalite could be preserved.

The Burdekin River Fault system and the Lynd Mylonite Zone (Palmerville Fault), which extend along the eastern and western margins of the Greenvale Province (Figure 1a), display many geological similarities to the Clarke River Fault. All three fault systems comprise Cambrian–Ordovician basement metamorphic rocks, of similar compositions, which were metamorphosed and deformed under comparable P–T conditions and structural styles (Arnold & Rubenach, 1976; Fergusson *et al.*, 2007a). Additionally,

fault-bound lenses of mafic–ultramafic rocks have been documented from within each fault system, and they are probably ophiolitic in origin. Cambrian–Ordovician subvolcanic porphyry intrusions have been documented across the Greenvale Province (Withnall *et al.*, 1991) but have not been found in the Running River Metamorphics. The preservation of shallow intrusive rocks and volcanics in the Greenvale Province indicates that the erosion level across the Greenvale Province is significantly shallower than across the Running River Metamorphics. The similarities in lithology, structural style and metamorphic facies between

the Greenvale Province and Running River Metamorphics, combined with preservation of the upper crust, make the Greenvale Province a compelling exploration target for early Paleozoic porphyry deposits.

Conclusions

Mafic–ultramafic rocks in the Running River Metamorphics yield an ophiolitic geochemical signature. The association of ophiolitic mafic–ultramafic rocks described in this paper and by Dirks *et al.* (2021), combined with metamorphic diamonds described by Edgar *et al.* (2022b), and concurrent, continental-arc-like intrusive bodies, suggests that the Clarke River Fault represents a continental suture zone. We constrain the genesis of the Falls Creek Tonalite to be subduction-related although probably emplaced during late syntectonism prior to the D4 deformation event that affected the Running River Metamorphics and the Falls Creek Tonalite. The geochemistry of the Falls Creek Tonalite is consistent with a fertile melt source; however, the mapped bodies were emplaced at mid-crustal depths considered too deep for the formation of porphyry ore deposits. Similar geology has been reported within the Greenvale Province, where the erosional level is much shallower, and the potential for undiscovered porphyry-style deposits is greater.

Acknowledgements

The authors would like to thank Kevin Blake, Yi Hu and Shane Askew from the Advanced Analytical Centre at James Cook University for their technical support during EPMA, and LA-ICP-MS data collection and processing. This manuscript was improved by the constructive reviews provided by David Purdy and an anonymous reviewer. Author contributions: AE and IS are responsible for conceptualisation, methodology, investigation, visualisation, supervision; AE wrote the original draft, and the writing, review and editing were carried out by all authors.

Disclosure statement

No potential conflict of interest was reported by the author(s).

Funding

The authors would like to thank the Geological Survey of Queensland for their funding of the research project. The first author would like to acknowledge the Australian Government Research Training Program Domestic Stipend Scholarship for financial support throughout this research, and the Economic Geology Research Centre (EGRU) at James Cook University for supporting this research. The authors would like to thank the Geological Survey of Queensland for their funding of the research project. The first author would like to acknowledge the Australian Government Research Training Program Domestic Stipend Scholarship for financial support throughout this research, and the Economic Geology Research Centre (EGRU) at James Cook University for supporting this research.

ORCID

A. Edgar  <http://orcid.org/0000-0002-8090-9788>
I. Sanislav  <http://orcid.org/0000-0002-3680-3740>
P. Dirks  <http://orcid.org/0000-0002-1582-1405>

Data availability statement

The authors confirm that the data supporting the findings of this study are available within the article or in the JCU Research Data repository <https://doi.org/10.25903/nf07-tv26>.

References

- Abdel-Karim, A-A M., Ali, S., Helmy, H. M., & El-Shafei, S. A. (2016). A fore-arc setting of the Gerf ophiolite, Eastern Desert, Egypt: Evidence from mineral chemistry and geochemistry of ultramafites. *Lithos*, 263, 52–65. <https://doi.org/10.1016/j.lithos.2016.05.023>
- Aitchison, J. C., & Buckman, S. (2012). Accordion vs. quantum tectonics: Insights into continental growth processes from the Paleozoic of eastern Gondwana. *Gondwana Research*, 22(2), 674–680. <https://doi.org/10.1016/j.gr.2012.05.013>
- Arai, S., & Akizawa, N. (2014). Precipitation and dissolution of chromite by hydrothermal solutions in the Oman ophiolite: New behavior of Cr and chromite. *American Mineralogist*, 99(1), 28–34. <https://doi.org/10.2138/am.2014.4473>
- Arnold, G. O., & Rubenach, M. J. (1976). Mafic-ultramafic complexes of the Greenvale area, North Queensland: Devonian intrusions or Precambrian metamorphics? *Journal of the Geological Society of Australia*, 23(2), 119–139. <https://doi.org/10.1080/00167617608728929>
- Barnes, S. J. (2000). Chromite in komatiites, II. Modification during greenschist to mid-amphibolite facies metamorphism. *Journal of Petrology*, 41(3), 387–409. <https://doi.org/10.1093/petrology/41.3.387>
- Barnes, S. J., & Roeder, P. L. (2001). The range of spinel compositions in terrestrial mafic and ultramafic rocks. *Journal of Petrology*, 42(12), 2279–2302. <https://doi.org/10.1093/petrology/42.12.2279>
- Belyaev, V., Gornova, M., Gordienko, I., Karimov, A., Medvedev, A. Y., Ivanov, A., Dril, S., Grigoriev, D., & Belozeroval, O. Y. (2021). Late Cambrian calc-alkaline magmatism during transition from subduction to accretion: Insights from geochemistry of lamprophyre, dolerite and gabbro dikes in the Dzhida terrain, Central Asian orogenic belt. *Lithos*, 386–387, 106044. <https://doi.org/10.1016/j.lithos.2021.106044>
- Buckman, S., Aitchison, J. C., Nutman, A. P., Bennett, V. C., Saktura, W. M., Walsh, J. M., Kachovich, S., & Hidaka, H. (2018). The Spongtag Massif in Ladakh, NW Himalaya: An Early Cretaceous record of spontaneous, intra-oceanic subduction initiation in the Neotethys. *Gondwana Research*, 63, 226–249. <https://doi.org/10.1016/j.gr.2018.07.003>
- Castillo, P. R., Janney, P. E., & Solidum, R. U. (1999). Petrology and geochemistry of Camiguin Island, southern Philippines: Insights to the source of adakites and other lavas in a complex arc setting. *Contributions to Mineralogy and Petrology*, 134(1), 33–51. <https://doi.org/10.1007/s004100050467>
- Cawood, P. A. (2005). Terra Australis Orogen: Rodinia breakup and development of the Pacific and Iapetus margins of Gondwana during the Neoproterozoic and Paleozoic. *Earth-Science Reviews*, 69(3–4), 249–279. <https://doi.org/10.1016/j.earscirev.2004.09.001>
- Chen, N., Pratt, W., Mao, J., Xie, G., Moisy, M., Santos, A., Guo, W., Zheng, W., & Liu, J. (2022). Geology and geochronology of the Miocene Rio Blanco Porphyry Cu–Mo Deposit, Northern Peru. *Economic Geology*, 117(5), 1013–1042. <https://doi.org/10.5382/econ-geo.4896;30>

- Chiaradia, M., Ulianov, A., Kouzmanov, K., & Beate, B. (2012). Why large porphyry Cu deposits like high Sr/Y magmas? *Scientific Reports*, 2(1), 685. <https://doi.org/10.1038/srep00685>
- Chung, S.-L., Liu, D., Ji, J., Chu, M.-F., Lee, H.-Y., Wen, D.-J., Lo, C.-H., Lee, T.-Y., Qian, Q., & Zhang, Q. (2003). Adakites from continental collision zones: Melting of thickened lower crust beneath southern Tibet. *Geology*, 31(11), 1021–1024. <https://doi.org/10.1130/G19796.1>
- Colás, V., González-Jiménez, J. M., Griffin, W. L., Fanlo, I., Gervilla, F., O'Reilly, S. Y., Pearson, N. J., Kerestedjian, T., & Proenza, J. A. (2014). Fingerprints of metamorphism in chromite: New insights from minor and trace elements. *Chemical Geology*, 389, 137–152. <https://doi.org/10.1016/j.chemgeo.2014.10.001>
- Cooke, D., Wilson, A., House, M., Wolfe, R., Walshe, J., Lickfold, V., & Crawford, A. (2007). Alkalic porphyry Au–Cu and associated mineral deposits of the Ordovician to early Silurian Macquarie Arc, New South Wales. *Australian Journal of Earth Sciences*, 54(2–3), 445–463. <https://doi.org/10.1080/08120090601146771>
- Crawford, A., Meffre, S., Squire, R. J., Barron, L., & Falloon, T. (2007). Middle and Late Ordovician magmatic evolution of the Macquarie Arc, Lachlan Orogen, New South Wales. *Australian Journal of Earth Sciences*, 54(2–3), 181–214. <https://doi.org/10.1080/08120090701227471>
- Defant, M. J., & Drummond, M. S. (1990). Derivation of some modern arc magmas by melting of young subducted lithosphere. *Nature*, 347(6294), 662–665. <https://doi.org/10.1038/347662a0>
- Defant, M. J., & Drummond, M. S. (1993). Mount St. Helens: Potential example of the partial melting of the subducted lithosphere in a volcanic arc. *Geology*, 21(6), 547–550. [https://doi.org/10.1130/0091-7613\(1993\)021%3C0547:MSHPEO%3E2.3.CO;2](https://doi.org/10.1130/0091-7613(1993)021%3C0547:MSHPEO%3E2.3.CO;2)
- Dewey, J. F. (1988). Extensional collapse of orogens. *Tectonics*, 7(6), 1123–1139. <https://doi.org/10.1029/TC007i006p01123>
- Dick, H. J. B., & Bullen, T. (1984). Chromian spinel as a petrogenetic indicator in abyssal and alpine-type peridotites and spatially associated lavas. *Contributions to Mineralogy and Petrology*, 86(1), 54–76. <https://doi.org/10.1007/BF00373711>
- Dilek, Y., & Furnes, H. (2014). Ophiolites and their origins. *Elements*, 10(2), 93–100. <https://doi.org/10.2113/gselements.10.2.93>
- Dirks, H. N., Sanislav, I. V., & Abu Sharib, A. S. A. A. (2021). Continuous convergence along the paleo-Pacific margin of Australia during the Early Paleozoic: Insights from the Running River Metamorphics, NE Queensland. *Lithos*, 398–399, 106343. <https://doi.org/10.1016/j.lithos.2021.106343>
- Edgar, A., Sanislav, I., & Dirks, P. (2022a). Tectonic setting and mineralisation potential of the Cowley Ophiolite Complex, north Queensland. *Australian Journal of Earth Sciences*, 69(8), 1132–1148. <https://doi.org/10.1080/08120099.2022.2086173>
- Edgar, A., Sanislav, I. V., Dirks, P. H., & Spandler, C. (2022b). Metamorphic diamond from the northeastern margin of Gondwana: Paradigm shifting implications for one of Earth's largest orogens. *Science Advances*, 8(27), eabo2811. <https://doi.org/10.1126/sciadv.abo2811>
- Fergusson, C. L., Henderson, R. A., Withnall, I. W., & Fanning, C. M. (2007a). Structural history of the Greenvale Province, north Queensland: Early Palaeozoic extension and convergence on the Pacific margin of Gondwana. *Australian Journal of Earth Sciences*, 54(4), 573–595. <https://doi.org/10.1080/08120090701188970>
- Fergusson, C. L., Henderson, R. A., Withnall, I. W., Fanning, C. M., Phillips, D., & Lewthwaite, K. J. (2007b). Structural, metamorphic, and geochronological constraints on alternating compression and extension in the early Paleozoic Gondwanan Pacific margin, north-eastern Australia. *Tectonics*, 26(3), N/A–N/A. <https://doi.org/10.1029/2006tc001979>
- Gamal El Dien, H., Arai, S., Doucet, L.-S., Li, Z.-X., Kil, Y., Fougereuse, D., Reddy, S. M., Saxey, D. W., & Hamdy, M. (2019). Cr-spinel records metasomatism not petrogenesis of mantle rocks. *Nature Communications*, 10(1), 1–12. <https://doi.org/10.1038/s41467-019-13117-1>
- George, R., Turner, S., Hawkesworth, C., Bacon, C. R., Nye, C., Stelling, P., & Dreher, S. (2004). Chemical versus temporal controls on the evolution of tholeiitic and calc-alkaline magmas at two volcanoes in the Alaska–Aleutian arc. *Journal of Petrology*, 45(1), 203–219. <https://doi.org/10.1093/petrology/egg086>
- Glen, R. A. (2013). Refining accretionary orogen models for the Tasmanides of eastern Australia. *Australian Journal of Earth Sciences*, 60(3), 315–370. <https://doi.org/10.1080/08120099.2013.772537>
- Glen, R. A., Belousova, E., & Griffin, W. L. (2016). Different styles of modern and ancient non-collisional orogens and implications for crustal growth: A Gondwanaland perspective. *Canadian Journal of Earth Sciences*, 53(11), 1372–1415. <https://doi.org/10.1139/cjes-2015-0229>
- Glen, R., Crawford, A., & Cooke, D. (2007). Tectonic setting of porphyry Cu–Au mineralisation in the Ordovician–Early Silurian Macquarie Arc, Eastern Lachlan Orogen, New South Wales. *Australian Journal of Earth Sciences*, 54(2–3), 465–479. <https://doi.org/10.1080/08120090701221672>
- Glen, R. A., Quinn, C., & Cooke, D. R. (2012). The Macquarie Arc, Lachlan Orogen, New South Wales: Its evolution, tectonic setting and mineral deposits. *Episodes*, 35(1), 177–186. <https://doi.org/10.18814/epiugs/2012/v35i1/017>
- Greenfield, J. E., Musgrave, R. J., Bruce, M. C., Gilmore, P. J., & Mills, K. J. (2011). The Mount Wright Arc: A Cambrian subduction system developed on the continental margin of East Gondwana, Koonenberry Belt, eastern Australia. *Gondwana Research*, 19(3), 650–669. <https://doi.org/10.1016/j.gr.2010.11.017>
- Harris, A. C., Cooke, D. R., Cuisson, A. L. G., Groome, M., Wilson, A. J., Fox, N., Holliday, J., & Tosdal, R. (2020). Geologic evolution of late Ordovician to early Silurian Alkalic Porphyry Au–Cu Deposits at Cadia, New South Wales, Australia. In R. H. Sillitoe, R. J. Goldfarb, F. Robert, & S. F. Simmons (Eds.), *Geology of the world's major gold deposits and provinces* (Chapter 30). Special Publication of the Society of Economic Geologists, 23. <https://doi.org/10.5382/SP.23.30>
- Henderson, R. (1986). Geology of the Mt Windsor subprovince—a lower Palaeozoic volcano-sedimentary terrane in the northern Tasman orogenic zone. *Australian Journal of Earth Sciences*, 33(3), 343–364. <https://doi.org/10.1080/08120098608729371>
- Henderson, R. A., & Fergusson, C. L. (2019). Growth and provenance of a Paleozoic subduction complex in the Broken River Province, Mossman Orogen: Evidence from detrital zircon ages. *Australian Journal of Earth Sciences*, 66(5), 607–624. <https://doi.org/10.1080/08120099.2019.1572033>
- Henderson, R. A., Fergusson, C. L., & Withnall, I. W. (2020). Coeval basin formation, plutonism and metamorphism in the Northern Tasmanides: Extensional Cambro-Ordovician tectonism of the Charters Towers Province. *Australian Journal of Earth Sciences*, 67(5), 663–680. <https://doi.org/10.1080/08120099.2020.1747539>
- Henderson, R. A., Innes, B. M., Fergusson, C. L., Crawford, A. J., & Withnall, I. W. (2011). Collisional accretion of a Late Ordovician oceanic island arc, northern Tasman Orogenic Zone, Australia. *Australian Journal of Earth Sciences*, 58(1), 1–19. <https://doi.org/10.1080/08120099.2010.535564>
- Hervé, M., Sillitoe, R. H., Wong, C., Fernández, P., Crignola, F., Ipinza, M., & Urzúa, F. (2012). Geologic overview of the Escondida porphyry copper district, northern Chile. In J. W., Hedenquist, M., Harris & F. Camus, (Eds.), *Geology and genesis of major copper deposits and districts of the world: A tribute to Richard H. Sillitoe* (Vol. 16, pp. 55–78). Society of Economic Geologists Special Publication.
- Huston, D. L., Taylor, T., Fabray, J., & Patterson, D. J. (1992). A comparison of the geology and mineralization of the Balcooma and Dry River South volcanogenic massive sulfide deposits, northern Queensland. *Economic Geology*, 87(3), 785–811. <https://doi.org/10.2113/gsecongeo.87.3.785>
- Irvine, T. N., & Baragar, W. (1971). A guide to the chemical classification of the common volcanic rocks. *Canadian Journal of Earth Sciences*, 8(5), 523–548. <https://doi.org/10.1139/e71-055>

- Kamenetsky, V., Crawford, A. J., & Meffre, S. (2001). Factors controlling chemistry of magmatic spinel: An empirical study of associated olivine, Cr-spinel and melt inclusions from primitive rocks. *Journal of Petrology*, 42(4), 655–671. <https://doi.org/10.1093/petrology/42.4.655>
- King, R. L., Kohn, M. J., & Eiler, J. M. (2003). Constraints on the petrological structure of the subduction zone slab-mantle interface from Franciscan Complex exotic ultramafic blocks. *Geological Society of America Bulletin*, 115(9), 1097–1109. <https://doi.org/10.1130/B25255.1>
- Klausen, M. B., Szilas, K., Kokfelt, T. F., Keulen, N., Schumacher, J. C., & Berger, A. (2017). Tholeiitic to calc-alkaline metavolcanic transition in the Archean Nigerlitasak Supracrustal Belt, SW Greenland. *Precambrian Research*, 302, 50–73. <https://doi.org/10.1016/j.precamres.2017.09.014>
- Kumar, A. A., Sanislav, I. V., Cathey, H. E., & Dirks, P. H. (2023). Geochemistry of indium in magmatic-hydrothermal tin and sulfide deposits of the Herberton Mineral Field, Australia. *Mineralium Deposita*, 1–20. <https://doi.org/10.1007/s00126-023-01179-7>
- Kumar, A. A., Sanislav, I. V., & Dirks, P. H. (2022). The geological setting of the indium-rich Baal Gammon and Isabel Sn–Cu–Zn deposits in the Herberton Mineral Field, Queensland, Australia. *Ore Geology Reviews*, 149, 105095. <https://doi.org/10.1016/j.oregeorev.2022.105095>
- Kuno, H. (1968). Differentiation of basalt magmas. In H. H. Hess & A. Poldervaart (Eds.), *Basalts: The Poldervaart treatise on rocks of basaltic composition* (pp. 623–688). Interscience Publishers.
- Kuşçu, İ., Tosdal, R. M., & Gençalioglu-Kuşcu, G. (2019). Porphyry-Cu deposits of Turkey. In F. Pirajno, T. Ünlü, C. Dönmez & M. B. Şahin (Eds.), *Mineral resources of Turkey* (pp. 337–425). Springer. <https://doi.org/10.1007/978-3-030-02950-0>
- Liu, H., Peng, T., & Guo, X. (2018). Geochronological and geochemical constraints on the coexistent N-MORB-and SSZ-type ophiolites in Babu area (SW China) and tectonic implications. *Journal of the Geological Society*, 175(4), 667–678. <https://doi.org/10.1144/jgs2017-121>
- Loucks, R. (2014). Distinctive composition of copper-ore-forming arc magmas. *Australian Journal of Earth Sciences*, 61(1), 5–16. <https://doi.org/10.1080/08120099.2013.865676>
- McDonough, W. F., & Sun, S-S. (1995). The composition of the Earth. *Chemical Geology*, 120(3–4), 223–253. [https://doi.org/10.1016/0009-2541\(94\)00140-4](https://doi.org/10.1016/0009-2541(94)00140-4)
- Miao, L., Fan, W., Liu, D., Zhang, F., Shi, Y., & Guo, F. (2008). Geochronology and geochemistry of the Hegenshan ophiolitic complex: Implications for late-stage tectonic evolution of the Inner Mongolia-Daxinganling Orogenic Belt, China. *Journal of Asian Earth Sciences*, 32(5–6), 348–370. <https://doi.org/10.1016/j.jseaes.2007.11.005>
- Moyen, J-F. (2009). High Sr/Y and La/Yb ratios: The meaning of the “adakitic signature”. *Lithos*, 112(3–4), 556–574. <https://doi.org/10.1016/j.lithos.2009.04.001>
- Mpodozis, C., & Cornejo, P. (2012). Cenozoic tectonics and porphyry copper systems of the Chilean Andes. In J. W. Hedenquist, M. Harris, F. Camus (Eds.), *Geology and genesis of major copper deposits and districts of the world: A tribute to Richard H. Sillitoe* (pp. 329–360). Society of Economic Geologists Special Publication, 16. <https://doi.org/10.5382/SP.16.14>
- Mullen, E. D. (1983). MnO/TiO₂/P₂O₅: A minor element discriminant for basaltic rocks of oceanic environments and its implications for petrogenesis. *Earth and Planetary Science Letters*, 62(1), 53–62. [https://doi.org/10.1016/0012-821x\(83\)90070-5](https://doi.org/10.1016/0012-821x(83)90070-5)
- Müntener, O., Kelemen, P. B., & Grove, T. L. (2001). The role of H₂O during crystallization of primitive arc magmas under uppermost mantle conditions and genesis of igneous pyroxenites: An experimental study. *Contributions to Mineralogy and Petrology*, 141(6), 643–658. <https://doi.org/10.1007/s004100100266>
- Murphy, J. B., van Staal, C. R., & Collins, W. J. (2011). A comparison of the evolution of arc complexes in Paleozoic interior and peripheral orogens: Speculations on geodynamic correlations. *Gondwana Research*, 19(3), 812–827. <https://doi.org/10.1016/j.gr.2010.11.019>
- Pearce, J. A. (2008). Geochemical fingerprinting of oceanic basalts with applications to ophiolite classification and the search for Archean oceanic crust. *Lithos*, 100(1–4), 14–48. <https://doi.org/10.1016/j.lithos.2007.06.016>
- Pearce, J. A., & Cann, J. R. (1973). Tectonic setting of basic volcanic rocks determined using trace element analyses. *Earth and Planetary Science Letters*, 19(2), 290–300. [https://doi.org/10.1016/0012-821x\(73\)90129-5](https://doi.org/10.1016/0012-821x(73)90129-5)
- Petford, N., & Atherton, M. (1996). Na-rich partial melts from newly underplated basaltic crust: The Cordillera Blanca Batholith, Peru. *Journal of Petrology*, 37(6), 1491–1521. <https://doi.org/10.1093/petrology/37.6.1491>
- Proenza, J. A., Zaccarini, F., Escayola, M., Cábana, C., Schalamuk, A., & Garuti, G. (2008). Composition and textures of chromite and platinum-group minerals in chromitites of the western ophiolitic belt from Pampean Ranges of Córdoba, Argentina. *Ore Geology Reviews*, 33(1), 32–48. <https://doi.org/10.1016/j.oregeorev.2006.05.009>
- Rapp, R. P., Watson, E. B., & Miller, C. F. (1991). Partial melting of amphibolite/eclogite and the origin of Archean trondhjemites and tonalites. *Precambrian Research*, 51(1–4), 1–25. [https://doi.org/10.1016/0301-9268\(91\)90092-0](https://doi.org/10.1016/0301-9268(91)90092-0)
- Richards, J. P. (2011). High Sr/Y arc magmas and porphyry Cu±Mo±Au deposits: Just add water. *Economic Geology*, 106(7), 1075–1081. <https://doi.org/10.2113/econgeo.106.7.1075>
- Richards, J. P., & Kerrich, R. (2007). Special paper: Adakite-like rocks: Their diverse origins and questionable role in metallogenesis. *Economic Geology*, 102(4), 537–576. <https://doi.org/10.2113/gsecongeo.102.4.537>
- Richards, J. P., Spell, T., Rameh, E., Razique, A., & Fletcher, T. (2012). High Sr/Y magmas reflect arc maturity, high magmatic water content, and porphyry Cu±Mo±Au potential: Examples from the Tethyan arcs of central and eastern Iran and western Pakistan. *Economic Geology*, 107(2), 295–332. <https://doi.org/10.2113/econgeo.107.2.295>
- Sajona, F. G., Maury, R. C., Pubellier, M., Leterrier, J., Bellon, H., & Cotten, J. (2000). Magmatic source enrichment by slab-derived melts in a young post-collision setting, central Mindanao (Philippines). *Lithos*, 54(3–4), 173–206. [https://doi.org/10.1016/S0024-4937\(00\)00019-0](https://doi.org/10.1016/S0024-4937(00)00019-0)
- Shervais, J. W. (1982). Ti–V plots and the petrogenesis of modern and ophiolitic lavas. *Earth and Planetary Science Letters*, 59(1), 101–118. [https://doi.org/10.1016/0012-821x\(82\)90120-0](https://doi.org/10.1016/0012-821x(82)90120-0)
- Shiraki, K. (1997). Geochemical behavior of chromium. *Shigen-Chishitsu*, 47(6), 319–330.
- Sillitoe, R. H. (2010). Porphyry copper systems. *Economic Geology*, 105(1), 3–41. <https://doi.org/10.2113/gsecongeo.105.1.3>
- Song, S., Niu, Y., Su, L., Zhang, C., & Zhang, L. (2014). Continental orogenesis from ocean subduction, continent collision/subduction, to orogen collapse, and orogen recycling: The example of the North Qaidam UHPM belt, NW China. *Earth-Science Reviews*, 129, 59–84. <https://doi.org/10.1016/j.earscirev.2013.11.010>
- Spandler, C., Hermann, J., Faure, K., Mavrogenes, J., & Arculus, R. (2008). The importance of talc and chlorite “hybrid” rocks for volatile recycling through subduction zones; evidence from the high-pressure subduction melange of New Caledonia. *Contributions to Mineralogy and Petrology*, 155(2), 181–198. <https://doi.org/10.1007/s00410-007-0236-2>
- Sun, W-d., Liang, H-y., Ling, M-x., Zhan, M-z., Ding, X., Zhang, H., Yang, X-y., Li, Y-l., Ireland, T. R., Wei, Q-r., & Fan, W-m. (2013). The link between reduced porphyry copper deposits and oxidized magmas. *Geochimica et Cosmochimica Acta*, 103, 263–275. <https://doi.org/10.1016/j.gca.2012.10.054>
- Sun, S-S., Nesbitt, R. W., & Sharaskin, A. Y. (1979). Geochemical characteristics of mid-ocean ridge basalts. *Earth and Planetary Science Letters*, 44(1), 119–138. [https://doi.org/10.1016/0012-821x\(79\)90013-X](https://doi.org/10.1016/0012-821x(79)90013-X)

- Sun, W., Zhang, H., Ling, M.-X., Ding, X., Chung, S.-L., Zhou, J., Yang, X.-Y., & Fan, W. (2011). The genetic association of adakites and Cu–Au ore deposits. *International Geology Review*, 53(5–6), 691–703. <https://doi.org/10.1080/00206814.2010.507362>
- Viereck, L., Flower, M., Hertogen, J., Schmincke, H.-U., & Jenner, G. (1989). The genesis and significance of N-MORB sub-types. *Contributions to Mineralogy and Petrology*, 102(1), 112–126. <https://doi.org/10.1007/BF01160195>
- Vos, I. M. A., Bierlein, F. P., & Teale, G. S. (2005). Genesis of orogenic-gold deposits in the Broken River Province, northeast Queensland. *Australian Journal of Earth Sciences*, 52(6), 941–958. <https://doi.org/10.1080/08120090500375190>
- Wells, T., Meffre, S., Cooke, D. R., Steadman, J., & Hoye, J. (2021). Assessment of magmatic fertility using pXRF on altered rocks from the Ordovician Macquarie Arc, New South Wales. *Australian Journal of Earth Sciences*, 68(3), 397–409. <https://doi.org/10.1080/08120099.2020.1782471>
- Winchester, J. A., & Floyd, P. A. (1977). Geochemical discrimination of different magma series and their differentiation products using immobile elements. *Chemical Geology*, 20(4), 325–343. [https://doi.org/10.1016/0009-2541\(77\)90057-2](https://doi.org/10.1016/0009-2541(77)90057-2)
- Withnall, I., Bain, J., Draper, J., MacKenzie, D., & Oversby, B. (1988). Proterozoic stratigraphy and tectonic history of the Georgetown Inlier, northeastern Queensland. *Precambrian Research*, 40–41, 429–446. [https://doi.org/10.1016/0301-9268\(88\)90079-4](https://doi.org/10.1016/0301-9268(88)90079-4)
- Withnall, I., Black, L., & Harvey, K. (1991). Geology and geochronology of the Balcooma area: Part of an Early Palaeozoic magmatic belt in North Queensland. *Australian Journal of Earth Sciences*, 38(1), 15–29. <https://doi.org/10.1080/08120099108727952>
- Withnall, I. W., & Henderson, R. A. (2012). Accretion on the long-lived continental margin of northeastern Australia. *Episodes*, 35(1), 166–176. <https://doi.org/10.18814/epiugs/2012/v35i1/016>
- Xiong, X., Adam, J., Green, T., Niu, H., Wu, J., & Cai, Z. (2006). Trace element characteristics of partial melts produced by melting of metabasalts at high pressures: Constraints on the formation condition of adakitic melts. *Science in China Series D: Earth Sciences*, 49(9), 915–925. <https://doi.org/10.1007/s11430-006-0915-2>
- Yao, J., Shu, L., & Santosh, M. (2014). Neoproterozoic arc-trench system and breakup of the South China Craton: Constraints from N-MORB type and arc-related mafic rocks, and anorogenic granite in the Jiangnan orogenic belt. *Precambrian Research*, 247, 187–207. <https://doi.org/10.1016/j.precamres.2014.04.008>
- Yellappa, T., Chetty, T. R. K., Tsunogae, T., & Santosh, M. (2010). The Manamedu Complex: Geochemical constraints on Neoproterozoic suprasubduction zone ophiolite formation within the Gondwana suture in southern India. *Journal of Geodynamics*, 50(3–4), 268–285. <https://doi.org/10.1016/j.jjog.2009.12.004>
- Yu, H., Zhang, H. F., Zou, H. B., & Yang, Y. H. (2019). Minor and trace element variations in chromite from the Songshugou dunites, North Qinling Orogen: Evidence for amphibolite-facies metamorphism. *Lithos*, 328–329, 146–158. <https://doi.org/10.1016/j.lithos.2019.01.009>
- Zhang, Q., Buckman, S., Bennett, V. C., & Nutman, A. (2019). Inception and early evolution of the Ordovician Macquarie Arc of eastern Gondwana margin: Zircon U–Pb–Hf evidence from the Molong volcanic belt, Lachlan Orogen. *Lithos*, 326–327, 513–528. <https://doi.org/10.1016/j.lithos.2019.01.008>
- Zheng, Y.-F., & Chen, R.-X. (2017). Regional metamorphism at extreme conditions: Implications for orogeny at convergent plate margins. *Journal of Asian Earth Sciences*, 145, 46–73. <https://doi.org/10.1016/j.jseaes.2017.03.009>
- Zheng, Y. F., Chen, R. X., Xu, Z., & Zhang, S. B. (2016). The transport of water in subduction zones. *Science China Earth Sciences*, 59(4), 651–682. <https://doi.org/10.1007/s11430-015-5258-4>